



Effects of miR-145-5p on cardiomyocyte proliferation and apoptosis, GIGYF1 expression and oxidative stress response in rats with myocardial ischemia-reperfusion

Changzai Liang¹, Shen Wang¹, Lijing Zhao², Yalei Han¹, Meng Zhang^{1,*}

¹Department of Cardiology, Aerospace Center Hospital, Beijing 100049, P.R. China

²Department of Cardiology, Luanping County Hospital, Chengde City 068250, Hebei Province, P.R. China

ARTICLE INFO

Original paper

Article history:

Received: October 28, 2021

Accepted: December 16, 2021

Published: January 30, 2022

Keywords:

miR-145-5p; GIGYF1; H2C2; cell proliferation; cell apoptosis; myocardial ischemia reperfusion; oxidative stress

ABSTRACT

This study aimed to investigate the effects of miR-145-5p on cardiomyocyte proliferation and apoptosis, GIGYF1 expression, inflammation, and oxidative stress in rats with myocardial ischemia-reperfusion injury (IRI). For this purpose, SPF male SD rats were used for IRI modeling. Experimental animals were subjected to specimen sampling and myocardial HE staining. The relative expression of miR-145-5p was detected by qRT-PCR; the protein expressions of GIGYF1, p-AKT, p53, Bax, p38MAPK, and ERK1/2 were detected by Western blot. Mouse embryonic cardiomyocytes H9C2 were used for H/R modeling, which was then subjected to cell transfection according to different grouping protocols. The target of miR-145-5p was confirmed to be GIGYF1 by dual-luciferase reporter assay. Further experiments were performed to detect the survival rate of transfected cells, the apoptosis of transfected cells, SOD activity determination, as well as IL-1 β and IL-6 concentrations. The results showed that the expression level of miR-145-5p was downregulated in H2C2 cells ($P < 0.05$). After 24h of transfection, there was a significant increase in the expression of miR-145-5p in the H/R+miR-145-5p mimic group ($P < 0.05$), but an evident decrease in the H/R+miR-145-5p inhibitor group ($P > 0.05$). Compared with the H/R+NC inhibitor group, the H/R+miR-145-5p mimic group had significantly increased cell proliferation, improved release of SOD, and upregulated expressions of ERK1/2 and p-AKT; but downregulated concentrations of IL-1 β and IL-6, and decreased expressions of P38MAPK, p53, and Bax (all $P < 0.05$). Also, the IRI+miR-145-5p agomir group had significantly upregulated expression of miR-145-5p and improved injury degree of heart tissue improved; a significant increase in the protein expressions ERK1/2 and p-AKT, but downregulated protein expressions of P38MAPK, p53, and Bax (all $P < 0.05$). Dual-luciferase reporter assay identified that GIGYF1 was the target gene of miR-145-5p. Furthermore, through the stimulated overexpression of miR-145-5p, there were significantly increased cell proliferation, improved release of SOD, and upregulated expressions of ERK1/2 and p-AKT; but downregulated concentrations of IL-1 β and IL-6, and decreased expressions of P38MAPK, p53, and Bax (all $P < 0.05$), while the above trends were reversed following the simultaneous upregulation of miR-145-5p and GIGYF1 (all $P < 0.05$). In general, our study confirmed a decreased expression of miR-145-5p and increased expression of GIGYF1 in the IRI or H/R model in vivo and in vitro. Overexpression of miR-145-5p can downregulate the expression of GIGYF1, further promote cell proliferation, inhibit cell apoptosis, alleviate inflammation and oxidative stress, and hence exert a protective role in myocardial infarction IRI.

DOI: <http://dx.doi.org/10.14715/cmb/2022.68.1.19> Copyright: © 2022 by the C.M.B. Association. All rights reserved.



Introduction

With the development of society and the change of lifestyle, the incidence rate of the human disease spectrum has gradually changed from infectious diseases to cancer and cardiovascular diseases (1). Acute myocardial infarction (AMI) has become one of the diseases with high morbidity and mortality (2). AMI is commonly treated by the recanalization of occluded vessels and rescuing myocardium in the ischemic marginal area (3). The specific measures include medicinal thrombolysis, percutaneous coronary intervention, coronary artery bypass

grafting, etc. (4, 5). However, after ischemia-reperfusion, there may be dysfunction of ischemic tissue, but also aggravated irreversible necrosis and apoptosis of myocardial cells in the ischemic area (6). There is even no-flow caused by microcirculation obstruction, which is ischemia-reperfusion injury (IRI) (7). Therefore, in addition to the degree of vascular recanalization, IRI has become another important factor affecting the therapeutic effect of AMI. The occurrence and development of IRI exhibit an intimate association with ischemia time, collateral circulation and cellular oxygen demand. During the development of AMI, an irreversible myocardial

*Corresponding author. E-mail: mengzhangmd@126.com
Cellular and Molecular Biology, 2022, 68(1): 147-159

injury may occur 20-30 minutes after subendocardial myocardial ischemia (8). The irreversible myocardial injury usually develops from endocardium to epicardium, which may be aggravated with time (9). The principle of prevention and treatment of IRI is to restore blood supply as soon as possible and take protective measures to reduce or even reverse cell damage (10, 11). It has been documented that the main mechanisms of IRI are free radical injury, intracellular calcium overload and leukocyte activation (12). Corresponding main protective measures are cytoprotective drugs, ischemic preconditioning, ischemic postconditioning, etc. (13, 14). Ischemic preconditioning and postconditioning are multiple transient ischemic treatments of myocardium before and after ischemia (14), which have the risk of operation and complications, and are mostly limited to the stage of animal experiment. Finding safe and effective cytoprotective agents to reduce IRI injury is the major focus of clinical treatment currently.

GRB10 interacting GYF protein 1 (GIGYF1) gene is located in 7q2, with a total length of about 10kb, which was discovered, together with GRB10 interacting GYF protein 2 (GIGYF2) by Barbara laboratory in 2003 (15). Both proteins can bind to the N-terminal of Grb10, and have a specific GYF domain. It has been reported that GIGYF1 was significantly expressed in myocardial tissue. In addition to binding to Grb10, GIGYF1 protein can also interact with AKT, EGFR and other factors to form macromolecular protein complex to regulate cell apoptosis (16), supporting its role in mediating the process of cell apoptosis. Meanwhile, Grb10 can activate tyrosine kinase receptors, including insulin growth factor receptor (IGF-1) and insulin receptor (17). Through binding to Grb10, GIGYF1 may regulate the insulin receptor signaling pathway, which can regulate the metabolic process of various nutrients *in vivo* and promote cell growth and proliferation (18). In addition, considering that Grb10 can promote the expression of downstream ERK1/2 to promote cell transcription and translation (17, 19). Therefore, GIGYF1 may indirectly regulate cell growth and proliferation by binding with Grb10. However, all the above regulatory processes remain to be validated and it is unclear with respect to the changes of cell proliferation and apoptosis after the alteration of

GIGYF1 expression. Importantly, recent research found that there was the loss of function variants in GIGYF1 gene, which were associated with type 2 diabetes and diseases with a series of complications such as cardiovascular diseases (20). It may suggest a possible association of GIGYF1 with the occurrence of cardiovascular diseases.

The miRNA is a class of small non-coding RNA with a length of about 22 nt (21). It can regulate the expression of specific target genes through complementary pairing at the transcriptional level, post-transcriptional level or epigenetic level. Under physiological or pathological conditions, multiple miRNAs also cooperate to form an RNA regulatory network to regulate cell growth, metabolism and apoptosis and affect the progress and prognosis of related diseases (21, 22). Recently, miRNA has been found to be involved in a variety of cardiovascular diseases, including heart failure, arrhythmia, myocardial hypertrophy, myocardial infarction, myocardial ischemia-reperfusion injury, etc. (23-25). At present, many miRNAs are involved in the process of ischemia-reperfusion, such as miR-24, miR-145, miR-211, etc. (26-28). These miRNAs play a complex regulatory role by acting on different target genes (26-29). Screening the key miRNAs regulating the expression of GIGYF1 can provide an important idea for clarifying the up-regulation mechanism of GIGYF1 and finding new endogenous cytoprotective agents.

So far, there is a lack of studies focusing on the role of miR-145-5p and GIGYF1 in IRI. Based on the above interpretation and speculation, this study established an animal model of myocardial ischemia-reperfusion in rats to explore whether miR-145-5p was the key miRNA regulating the expression of GIGYF1 after myocardial ischemia-reperfusion, so as to provide a new theoretical basis for the pathogenesis of IRI. Besides, this study further explored whether the regulation of miR-145-5p could provide a protective effect in the rat model of ischemia-reperfusion, so as to provide an experimental basis for endogenous prevention and treatment of IRI.

Materials and methods

Experimental model establishment

A total of 40 SPF male SD rats weighing 250-300g were raised in the animal experiment center of The First Affiliated Hospital, and College of Clinical Medicine of Henan University of Science and Technology. The feeding environment was clean and the temperature was maintained at 20-22°C. The animals were raised in cages, with 2 animals in each cage, fed with standard feed, with free access to drinking water, bedding change and cage disinfecting twice a week. The use of animals complied with the regulations of the animal management committee of The First Affiliated Hospital, and College of Clinical Medicine of Henan University of Science and Technology. Experimental animals were randomly divided into two groups, with 10 rats in each group. The first group was the sham group (n=10), and SD rats received thoracotomy only without ligation of the anterior descending coronary artery and were killed 6 h later. The second group was the modeling group (n=30), namely, IRI group. SD rats were subject to thoracotomy for IR and killed 2h later.

The rats were fed adaptively for one week after purchase. After intraperitoneal injection of 10% chlorine hydrate (350mg/kg) for anesthesia, the rats were fixed in the supine position after no righting reaction was observed. After cutting off the hair on the neck and chest, rats were disinfected with complexing iodine 3 times. Under sterile conditions, the neck skin was cut, followed by passive separation of the neck muscles, exposure of the trachea, cutting open the trachea laterally for 2-3mm at 0.5cm below the thyroid gland, and connection the intubation to the small animal ventilator. After cutting the left chest skin, the muscles were bluntly separated, followed by the exposure of the third and fourth auxiliary bones longitudinally, tearing of the pericardium and exposure of the heart. At 1-2mm below the junction of pulmonary conus and aorta, a loose knot was made in the anterior descending branch of the left coronary artery with 5-0 sliding thread with a suture needle. The successful signs of complete occlusion of the anterior descending coronary artery were that the myocardium below the ligation site turned pale, the pulse weakened, and the ST segment of ECG increased significantly. After 45 min of ischemia, the knot was untied and the blood flow of the anterior descending branch was restored. After 30 min of observation, the chest was closed with negative pressure; the chest wall and skin were sutured layer by layer, followed by the

withdrawal of the ventilator, suture of the neck skin collaterals and iodine disinfection of the incision. Each rat was injected intraperitoneally with 100,000 units of penicillin g every day to prevent infection for 3 consecutive days.

In addition to sham group as normal control, another 30 IRI rats were randomly divided into three groups: IRI group (intramyocardial injection of normal saline as control) and IRI + agomir NC group (intramyocardial injection of 100 µl agomir-NC), IRI + miR-145-5p group (intramyocardial injection of 100 µl miR-145-5p agomir), with injection every 3 days for 3 weeks. After treatment, they were placed in the feeding center for subsequent experiments.

Specimen sampling and myocardial HE staining

Before the rats were to be killed, the rats were anesthetized by intraperitoneal injection of 10% chloral hydrate (35mg/kg), the coronary artery was ligated again. An amount of 4ml 1% Evans blue was injected into the left ventricular cavity through the apex of the heart, the heart was cut off immediately, washed with ice normal saline. The ischemic area was white and the non-ischemic area was dyed blue. The large blood vessels, atrium and right ventricular tissues were cut off (ice operation), and water of the tissues was sucked with sterile filter paper. The heart was transected into two halves at the middle point perpendicular to the long axis of the left ventricle of the heart. The apical part was fixed with 4% paraformaldehyde for 8 ho and then preserved with sodium azide for morphological examination. Part of the ischemic and non-ischemic tissues in the heart bottom was put into the cryopreservation tube. After quick freezing with liquid nitrogen, tissues were transferred to the - 80°C ultra-low temperature refrigerator for preservation and kept for molecular biology detection.

During the HE staining, the apical part was dehydrated with alcohol and embedded in paraffin. The paraffin-embedded tissue was then continuously sectioned with a thickness of 4 µm and preserved at 37°C overnight. After conventional dewaxing and hydration, the sections were placed in hematoxylin solution for 10min, 0.5% hydrochloric acid solution for 10s, water washing for 20min, 0.5% eosin alcohol solution for 1min and 95% alcohol for 30s. Then, the sections were dried in the oven, placed in 100% alcohol I for 5min, 100% alcohol II for 5min, xylene I for 5min,

xylene II for 5min, and sealed with neutral gum. Meanwhile, TTC staining was also performed to reflect the infarct size changes in relative to the total size.

Detection of the relative expression of miR-145-5p by qRT-PCR

Every 100mg tissue specimen was added with 1 ml Trizol reagent and fully homogenized on ice, followed by the gentle blowing of the cells with a pipette tip. The homogenized tissue sample was put into an Eppendorf tube, added with 0.2ml chloroform, fully mixed and placed at room temperature for 5min. Centrifugation was performed at 12,000rpm at 4 °C for 15min to suck the supernatant, followed by another centrifugation similarly, with the supernatant removed and the precipitation saved. Then, 1ml of 75% pre-cooled ethanol was added for washing of the precipitated RNA by shaking. With another centrifugation at 7,500rpm for 5min and absorption of the supernatant, the precipitated samples were dried with air for 10min. After the addition of 20 μ l DEPC solution for full dissolving, RNA integrity was detected and the DNA in RNA was digested, which was then stored in the refrigerator at - 20°C. In the next step of reverse transcription synthesis of cDNA, 1 μ l Oligo dT and 5.0 μ g Total RNA were added into the tube, supplemented with DEPC solution to 12 μ l, which was mixed well, centrifuged and placed in a warm bath at 65°C for 5min. For miR-145-5p detection, the reaction system was prepared according to the following scheme (on ice): 5 \times Reaction Buffer 5 μ l; Total RNA 18 μ l (1-5 μ g); 2.5 U/ μ l Poly A Polymerase 1 μ l; RT Mix 1 μ l; Total volume: 25 μ l. After mixing, the cDNA was stored in the freezer at - 20°C by transient centrifugation. The above system was reacted at 37 °C for 1 h, and then at 85 °C for 5 min. For amplification of real-time PCR, the gene sequence was consulted from Genbank and designed by software Primer 5.0 according to the primer design principle. The reaction system of miR-145-5p was: cDNA 1 μ l; miR-145-5p or U6 primers 4 μ l; 50 \times ROX Reference Dye 0.4 μ l; 2 \times All-in-one-qPCR 10 μ l; H₂O 4.6 μ l; Total volume: 20 μ l. For the relative quantitative analysis of PCR products, after the PCR amplification reaction, the baseline and threshold were adjusted in the experimental system, and the number of cycles to achieve the threshold value was Ct of each reaction well. Relative expression of the target gene was

calculated based on the formula of $2^{-\Delta\Delta Ct}$ ($\Delta Ct = Ct_{miR-145-5p} - Ct_{U6}$). The steps of cell detection were the same as those of tissue detection.

Detection of the protein expressions of GIGYF1, p-AKT, p53, Bax, p38MAPK and ERK1/2 by Western blot

In the preparation of the protein sample, 0.25g of tissue to be tested was cut into EP tube and protein lysate was added. The lysed sample was placed at 4°C and shaken violently up and down for 6 times for 1 min each time, followed by centrifugation at 4°C at a centrifugal speed of 12000rpm for 20min. The supernatant was sucked and transferred in separate tubes for further storage. Bradford method was used to detect protein concentration and SDS-PAGE gel electrophoresis was performed. The tested sample was put into the EP tube and a 2 \times SDS loading buffer was added. The initial voltage of electrophoresis was 80V. When bromophenol blue entered the separation gel, the voltage was adjusted to 120V. Electrophoresis was terminated after 3h. After PVDF membrane transfer, antibody incubation and development were carried out. To be specific, after sealing at 4°C overnight with 5% skimmed milk powder, prepared with TBS, the primary antibodies were added for incubation at 37°C for 1h. With the primary antibodies discarded and rinsing with TBST for 10min each time, three times in total, a goat anti-rabbit secondary antibody was added for incubation at 37°C for 45 min. The secondary antibody was discarded and repeated washing with TBST was performed. The development was conducted with ECL in dark for 3min. After rinsing, the films were scanned and the images were analyzed by image analysis system IPP6.0. The steps of cell detection were the same as those of tissue detection.

Culture of rat cardiomyocytes

The purchased mouse embryonic cardiomyocytes H9C2 were added with DMEM culture medium containing 10% fetal bovine serum, cultured in a 75cm² culture flask at 37°C and 5% CO₂ incubator, and the solution was changed every 3-5 days. After absorbing the old medium, 1mL of trypsin containing 0.25% was added for digestion. After cell wall detachment under the microscope, 3mL of complete medium was added immediately to terminate digestion. The culture medium was then transferred into a 15mL centrifuge

tube, centrifuged at 1,000rpm for 5min. With the removal of the supernatant, a 6 mL fresh DMEM complete medium was added for the preparation of cell suspension via blowing repeatedly. After counting with a blood cell counter, cells were inoculated and cultured continuously at the cell density of 1×10^5 cells/well in a 6-well plate. Subsequent experiments were performed when the cell fusion was 50% - 60%.

Cell hypoxia/reoxygenation (H/R) treatment: H9C2 cells with good growth were added to DMEM culture medium without serum and antibiotics for 12h. After that, cells were continued to be cultured in a 1%O₂-94%N₂-5%CO₂ incubator at 37°C for 4h. Then cells were taken out with the original culture medium discarded, followed by culture with DMEM complete medium containing 10% fetal bovine serum in 5%CO₂ incubator at 37°C for 3h.

Experimental grouping and cell transfection

Cell grouping was performed according to the following protocols: (A) Control group without the addition of miR-145-5p mimic or inhibitor, but with Opti-MEM1 and LipofectamineTM2000 transfection reagent; (B) mimic NC group with the addition of 100nM mimic NC, and Opti-MEM1 diluted LipofectamineTM2000 reagent; (C) inhibitor NC group with the addition of 100nM inhibitor NC, and Opti-MEM1 diluted LipofectamineTM2000 reagent; (D) miR-145-5p mimic group with the addition of 100nM miR-145-5p mimic, and Opti-MEM1 diluted LipofectamineTM2000 reagent; and (E) miR-145-5p inhibitor with the addition of 100nM miR-145-5p inhibitor, and Opti-MEM1 diluted LipofectamineTM2000 reagent.

H9C2 cells were transfected according to the instructions of the LipofectamineTM2000 transfection reagent. The well-growing H9C2 cells were digested and inoculated at a cell density of 5×10^4 cells/well in 6-well plates, cultured in DMEM medium without serum and antibiotics for 24 h, and transfected when the cell fusion reached 50%. After transfection for 12 h, the cell supernatant was aspirated and cells were washed with sterile PBS 2 times. After each well was added with 2.5ml DMEM complete medium containing 10% fetal bovine serum, the cells were retained for detection after 24 h.

Dual-luciferase reporter assay

The target of miR-145-5p was confirmed to be GIGYF1 by dual-luciferase reporter assay. The 3'UTR GIGYF1 was synthesized, artificially, and the pCDNA3-Luc reporter gene vector of GIGYF1 was constructed based on pCDNA3.0. The luciferase gene sequence was amplified with pGEM-Luc as a template and inserted between Hind III and Kpn I sites of the pCDNA3.0 vector. Luciferase plasmids pRL-TK-GIGYF1 WT and pRL-TK-GIGYF1 MUT were transfected into cells with miR-145-5p mimic and NC mimic. After transfection for 12 h, DMSO was added for 24 h of treatment, and different groups of cells were collected for subsequent washing with $1 \times$ PBS. After that, the cells were lysed with the buffer of the dual-luciferase reporter assay kit, and the luciferase activity was detected with Glomax20/20 luminometer fluorescence detector. Each experiment was repeated three times.

CCK8 to detect the survival rate of transfected cells

According to the experimental grouping, each group was set with 6 multiple wells. H9C2 cardiomyocytes in the logarithmic growth stage were digested into cell suspension, which was then spread in three 96-well plates at a cell density of 5×10^3 cells/mL with 100 μ l cell suspension per well. After 24 hours of treatment, the cells were transfected for 12h. After that, the liquid was removed, cells were washed with PBS twice, and a fresh DMEM complete medium was added for subsequent culture. When the cells were cultured for 24h, 10 μ l of CCK8 solution was added under the condition of 37°C for 2h. The absorbance value of each well was detected at the wavelength of 450nm with Microplate Reader.

Flow cytometry to detect the apoptosis of transfected cells

After transfection for 12 h and continued culture for 48 h, the culture medium was removed and cells were washed twice with 3mL PBS. Then, 300 μ l trypsin without EDTA was used to digest the cells. When there was an obvious gap between the cells, the trypsin was removed and DMEM medium containing fetal bovine serum was added, after which centrifugation was performed at 1000r/min for 5min. The supernatant was removed after centrifugation. With the addition of 3mL PBS, cells were centrifuged at 1000r/min for 5min, and then 300 μ l PBS buffer was added to re-suspend the

cells. Subsequently, 5 μ l Annexin V-FITC and 10 μ lPI were added into 100 μ l cell suspension, respectively. When extracting the cell suspension, pay attention to shaking the cell suspension evenly. After all the solutions were added, the solution was placed in the dark for 15min, followed by the addition of 400 μ l PBS to detect cell apoptosis on the flow cytometer.

SOD activity determination

After H9C2 cell incubation with the addition of H₂O₂, superoxide anion free radicals were produced by the xanthine-xanthine oxidase system. The activity of SOD was detected through the measurement of the inhibition rate of SOD at the wavelength of 550 nm.

ELISA assay to detect IL-1 β and IL-6 concentrations

Inflammatory factors IL-1 β and IL-6 concentrations were determined in cell culture supernatant according to the instructions of the ELISA assay kit as described in prior literature in conventional steps (30). Corresponding absorbance values were detected in a Microplate Reader at a wavelength of 450 nm within 3 min of detection.

Statistical analysis

The statistical analysis of all data and plotting of all data graphs in our experiment was realized by using GraphPad Prism 8.0 (GraphPad Software Inc., La Jolla, CA, USA). All experiments were repeated at least 3 times. All data were consistent with normal distribution and examined by variance homogeneity test. The measurement data were expressed in the form of mean \pm standard deviation. The comparison between the two groups was achieved with an independent sample t-test, the comparison of multiple groups of data was analyzed by one-way analysis of variance, and Tukey's test was used for post hoc test. $P < 0.05$ was used to present the presence of a statistically significant difference.

Results and discussion

Intervention on miR-145-5p expression inhibited excessive apoptosis, promoted cell proliferation, and improved H/R injury of cardiomyocytes *in vitro*

Our study proposed a hypothesis that miR-145-5p might play a role in the process of cardiomyocyte H/R and cardiomyocyte proliferation and apoptosis. In order to detect the effect of miR-145-5p on H/R injury of rat cardiomyocytes in the process of H/R cell model

and cardiomyocyte proliferation and apoptosis, the H9C2 cell H/R model was established, and the expression of miR-145-5p was detected by qRT-PCR. According to the results (Figure 1A), compared with the control group, the expression level of miR-145-5p in H9C2 cells was downregulated in the H/R group ($P < 0.05$). Furthermore, the H9C2 cell model was treated with miR-145-5p overexpression and silencing, and the transfection efficiency was detected by qRT-PCR. It was found that after 24h of transfection, there was a significant increase in the expression of miR-145-5p in the H/R+miR-145-5p mimic group ($P < 0.05$), but an obvious decrease in its expression in the H/R+miR-145-5p inhibitor group ($P < 0.05$; Figure 1B).

Meanwhile, CCK8 assay and flow cytometry were performed to detect cell proliferation and apoptosis, SOD test was used to detect the release ability of superoxide dismutase, and ELISA test was used to detect IL-1 β and IL-6 in the supernatant of culture medium, besides, proliferation and apoptosis-related proteins were detected by Western blot. It can be observed that compared with the H/R+NC mimic group, H/R+miR-145-5p mimic group had significantly increased cell proliferation (Figure 1C), improved release of SOD (Figure 1E), and upregulated expressions of ERK1/2 and p-AKT (Figure 1G); but suppressed cell apoptosis (Figure 1D), evidently downregulated concentrations of IL-1 β and IL-6 (Figure 1FG), and decreased expressions of P38MAPK, p53 and Bax (Figure 1G) (all $P < 0.05$). While through the silencing of the expression of miR-145-5p, there were decreased cell proliferation (Figure 1C), the reduced release of SOD (Figure 1E), and downregulated expressions of ERK1/2 and p-AKT (Figure 1G); but obviously promoted cell apoptosis (Figure 1D), evidently increased concentrations of IL-1 β and IL-6 (Figure 1FG), and upregulated expressions of P38MAPK, p53 and Bax (Figure 1G) in H/R+miR-145-5p mimic group (all $P < 0.05$).

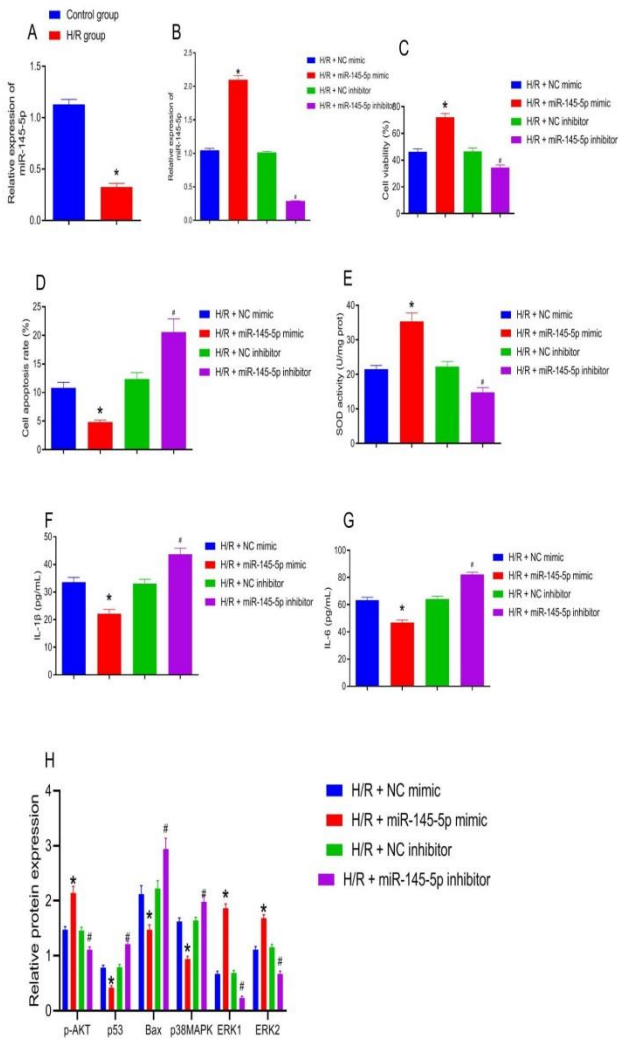


Figure 1. Intervention on miR-145-5p expression inhibited excessive apoptosis, promoted cell proliferation, and improved H/R injury of cardiomyocytes *in vitro*. Note: A. qRT-PCR detection of the expressions of miR-145-5p in the control group and model group. After constructing the H/R model of H9C2 cells, miR-145-5p mimic or miR-145-5p inhibitor was transfected into H9C2 cells. B. qRT-PCR detection of the expressions of miR-145-5p in H9C2 cells; C. CCK8 detection of cell proliferation of H9C2 cells; D. Flow cytometry detection of cell apoptosis of H9C2 cells; E. SOD test for detecting the release activity of superoxide dismutase in H9C2 cells; ELISA assay for detecting IL-1 β (F) and IL-6 (G) in the supernatant of culture medium; H. Western blot detection of p-AKT, p53, Bax, p38MAPK and ERK1/2 protein expressions in H9C2 cells. n = 3. Data were expressed by mean \pm SD, * P < 0.05. Statistical analysis was performed by using Student's t-test and with three repeated procedures for each experiment.

Intervention on miR-145-5p expression alleviated myocardial IRI *in vivo*

As described above, miR-145-5p could alleviate H/R-induced cardiomyocyte inflammation, proliferation and apoptosis *in vitro*. For further exploration of the regulatory effect of miR-145-5p myocardial ischemia-reperfusion in a rat model, the degree of myocardial injury was detected by the HE staining. It was found that compared with the sham group, inflammatory cells infiltrated and ruptured in the IRI group, and extensive fibrous scar tissue was formed in the infarct area and infarct edge area, showing severe myocardial necrosis (Figure 2A). TTC staining detected the size of myocardial infarction after myocardial ischemia (Figure 2B) and observed that compared with the sham group, the myocardial infarction area in the IRI group was larger.

In our subsequent experiment, lentivirus vectors lv-miR-145-5p agomir and negative control lv-agomir-NC were injected into the IRI rat model. qRT-PCR was used to detect the expression level of miR-145-5p in cardiac organs of different treatment groups, and it was detected that the IRI+miR-145-5p agomir group had significantly upregulated expression of miR-145-5p when compared with those in the IRI+agomir-NC group (both P < 0.05; Figure 2C). Further results of HE staining and TTC staining also showed that the injury degree of heart tissue improved in the IRI+miR-145-5p agomir group (Figure 2AB). Furthermore, there was a significant increase in the protein expressions of ERK1/2 and p-AKT but downregulated protein expressions of P38MAPK, p53 and Bax (all P < 0.05; Figure 2D). These results suggested that in the IRI rat model, overexpressing miR-145-5p could narrow the infarct size, inhibit excessive apoptosis, promote cell proliferation, and improve myocardial IRI.

Identification of GIGYF1 as the target gene of miR-145-5p

The binding site of miR-145-5p and GIGYF1 was obtained from TargetScan (Figure 3A). Therefore, we proposed a hypothesis that miR-145-5p might regulate IRI by targeting GIGYF1 to affect cardiomyocyte proliferation and apoptosis.

Firstly, a dual-luciferase reporter assay was carried out to identify whether GIGYF1 was the target gene of miR-145-5p. As shown in Figure 3B, compared with NC mimic+GIGYF1-3'UTR WT co-transfection group, the miR-145-5p mimic+GIGYF1-3'UTR WT co-transfection group had significantly reduced fluorescence intensity (P < 0.05). While no significant

statistical difference was observed when compared miR-145-5p mimic+GIGYF1-3'UTR MUT co-transfection group with NC mimic+GIGYF1-3'UTR MUT co-transfection group ($P > 0.05$). Their results supported that miR-145-5p specifically binds to GIGYF1 gene expression.

by mean \pm SD, *compared with sham group, $P < 0.05$; #compared with IRI+agomir-NC group, $P < 0.05$. Statistical analysis among groups was performed by using one-way analysis of variance and Tukey's test was used for post hoc test.

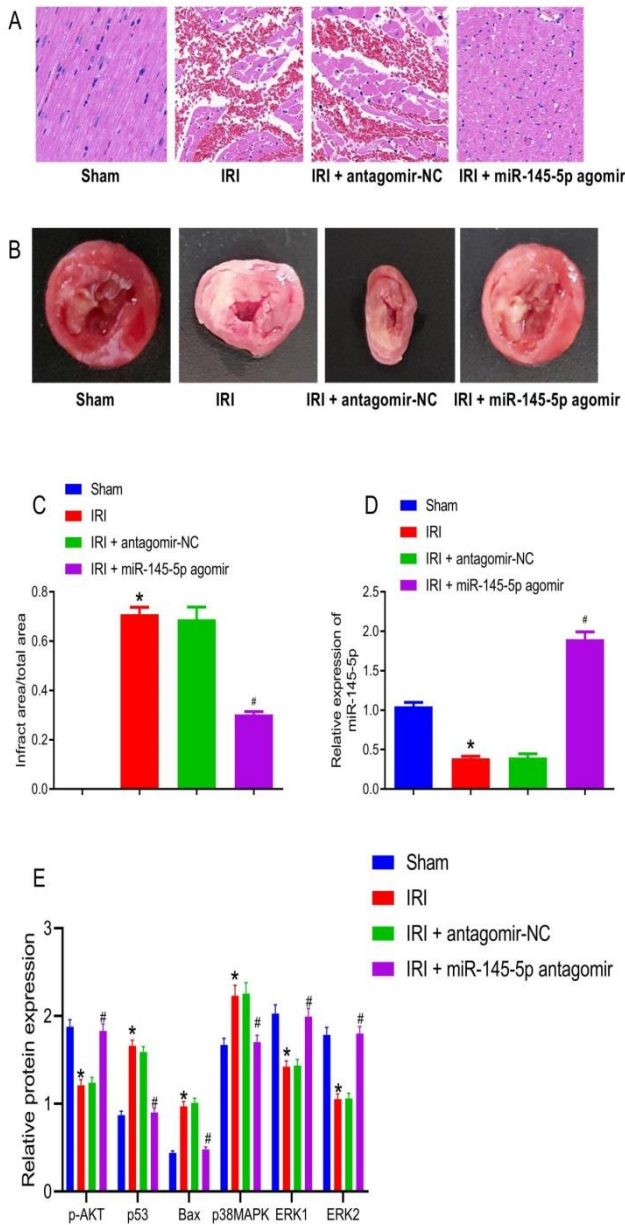


Figure 2. Intervention on miR-145-5p expression alleviated myocardial IRI *in vivo*. Note: The IRI rat model was established and lv-miR-145-5p agomir or lv-agomir-NC was injected into the myocardium of the IRI rat model. A. HE staining of the degree of myocardial tissue injury in different groups (Scale bar = 100 μ m); B. TTC staining of the infarct area of rat heart; C. qRT-PCR detection of the expression of miR-145-5p in different groups; D. Western blot detection of p-AKT, p53, Bax, p38MAPK and ERK1/2 protein expressions in different groups. n = 10. Data were expressed

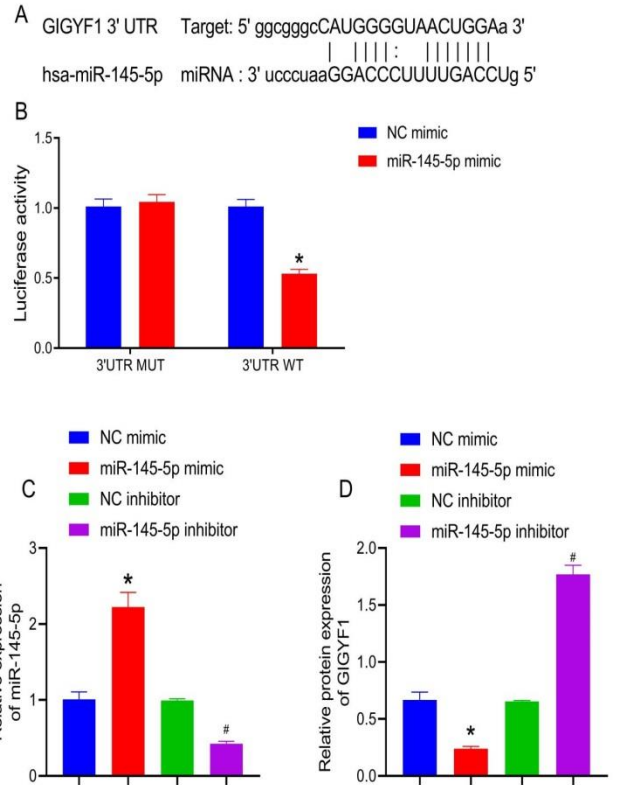


Figure 3. Identification of GIGYF1 as the target gene of miR-145-5p. Note: A. Binding site of miR-145-5p and GIGYF1 obtained by TargetScan; B. The binding of miR-145-5p to GIGYF1 was detected by dual-luciferase reporter assay. The miR-145-5p mimic and miR-145-5p inhibitor were transfected into H9C2 cells. C. qRT-PCR detection of the transfection efficiency; D. Western blot detection of the expression of GIGYF1 in H9C2 cells. n = 3. Data were expressed by mean \pm SD, * $P < 0.05$, ** $P < 0.01$, *** $P < 0.001$. Statistical analysis was performed by using Student's t-test and with three repeated procedures for each experiment.

At the same time, miR-145-5p was overexpressed or silenced in H9C2 cells, and the transfection efficiency was detected by qRT-PCR. Consequently, after 24h of transfection, the miR-145-5p mimic group showed significantly increased expression of miR-145-5p, while the miR-145-5p inhibitor group revealed decreased expression of miR-145-5p (both $P < 0.05$; Figure 3C). Simultaneously, according to the detection of GIGYF1 protein expression by using Western blot (Figure 3D), the expression of GIGYF1 was significantly downregulated in H9C2 cells of the miR-

145-5p mimic group, whereas GIGYF1 expression was highly upregulated in the miR-145-5p inhibitor group (both $P < 0.05$). Collectively, GIGYF1 was a direct binding target of miR-145-5p, and miR-145-5p could inhibit the expression of GIGYF1.

Intervention on miR-145-5p expression inhibited excessive apoptosis, promoted cell proliferation, and improved H/R injury of cardiomyocytes *in vitro* via targeting GIGYF1

In order to explore the mechanism of miR-145-5p regulating H/R injury, we first constructed the H/R model of H9C2 cells, and the expression of GIGYF1 was upregulated in H9C2 cells, and the transfection efficiency was detected by Western blot. After 24h of transfection, there was remarkably upregulated expression in the H/R+oe-GIGYF1 group (Figure 4A).

To verify whether miR-145-5p inhibited cardiomyocyte excessive apoptosis, promotes cell proliferation, and then improves H/R injury by targeting GIGYF1, we treated H9C2 cells with miR-145-5p mimic alone or miR-145-5p mimic and oe-GIGYF1 together. Western blot was used to detect the expression of GIGYF1 in H9C2 cells. It was noticed that the expression of GIGYF1 was downregulated after overexpression of miR-145-5p; whereas the role of miR-145-5p on GIGYF1 was reversed following simultaneous overexpression of miR-145-5p and GIGYF1 (Figure 4B). Furthermore, CCK8 assay and flow cytometry were performed to detect cell proliferation and apoptosis, SOD test was used to detect the release ability of superoxide dismutase, and ELISA test was used to detect IL-1 β and IL-6 in the supernatant of culture medium, and Western blot was used to detect the protein expressions of p-AKT, p53, Bax, p38MAPK and ERK1/2. Through the stimulated overexpression of miR-145-5p, there were significantly increased cell proliferation (Figure 4C), the improved release of SOD (Figure 4E), and upregulated expressions of ERK1/2 and p-AKT (Figure 4HI); but inhibited cell apoptosis (Figure 4D), evidently downregulated concentrations of IL-1 β and IL-6 (Figure 4FG), and decreased expressions of P38MAPK, p53 and Bax (Figure 4HI) (all $P < 0.05$), while the above trends were reversed following the simultaneous upregulation of miR-145-5p and GIGYF1 (all $P < 0.05$). With respect to the above, downregulation of miR-145-5p could upregulate the

expression of GIGYF1 targeted, which could inhibit excessive apoptosis of cardiomyocytes, promote cell proliferation, resulting in the alleviated myocardial H/R injury.

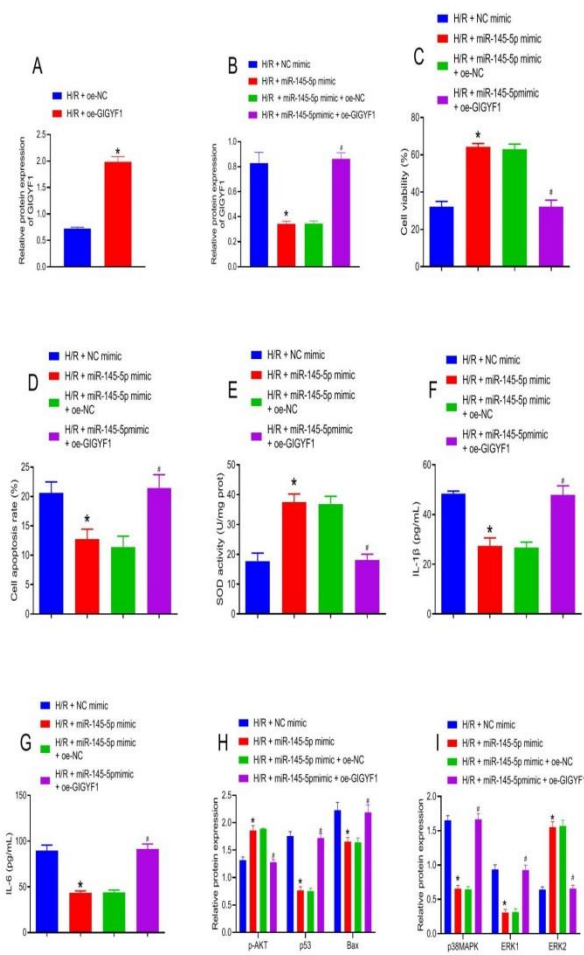


Figure 4. Intervention on miR-145-5p expression inhibited excessive apoptosis, promoted cell proliferation, and improved H/R injury of cardiomyocytes *in vitro* via targeting GIGYF1. Note: A. Western blot detection of the expressions of H9C2 in control and model cells. B. Western blot detection of the expressions of GIGYF1 in H9C2 cells after overexpression of GIGYF1. miR-145-5p mimic alone or miR-145-5p mimic and oe-GIGYF1 were transfected into H9C2 cells at the same time. C. Western blot detection of the expressions of GIGYF1 in H9C2 cells; D. CCK8 detection of cell proliferation of H9C2 cells; E. Flow cytometry detection of cell apoptosis of H9C2 cells; F. SOD test for detecting the release activity of superoxide dismutase in H9C2 cells; ELISA assay for detecting IL-1 β (G) and IL-6 (H) in the supernatant of culture medium; I. Western blot detection of p-AKT, p53, Bax, p38MAPK and ERK1/2 protein expressions in H9C2 cells. n = 3. Data were expressed by mean \pm SD, * $P < 0.05$, ** $P < 0.01$, *** $P < 0.001$. Statistical analysis between groups was conducted by using Student's t-test; Statistical analysis among groups was

performed by using one-way analysis of variance and Tukey's test was used for post hoc test.

In our study, through the establishment of an animal model of IRI and H2C2 cell model of H/R, our study confirms the protective role of miR-145-5p and GIGYF1 in IRI, providing a novel theoretical basis for the pathogenesis and treatment of IRI. So far, there is a lack of research concerning the mediating role of miR-145-5p and GIGYF1 in affecting the development of myocardial IRI to exert a protective effect, our study carried out basic research from the aspects of preventing cell apoptosis, promoting cell proliferation, and alleviating oxidative stress.

The development of bioinformatics provides a great tool for predicting the corresponding miRNA by detecting the 3'-UTR sequence of target mRNA (31). According to the commonly used prediction software Targets can, we found that a variety of miRNAs may regulate the expression of GIGYF1. More importantly, miR-145 has been recognized to be a key mediator in the occurrence and development of cardiovascular diseases, which has been confirmed to play a role in myocardial IRI. For instance, Hu *et al.* (32) reported that FGF21 protects myocardial cells against IRI injury by promoting an increase in miR-145 levels and autophagy while inhibiting Angpt2 expression, suggesting a novel therapeutic strategy for protecting against myocardial IRI injury. Lin *et al.* (33) suggested that through the involvement of (-)-epigallocatechin gallate, an increase in miR-145 may ameliorate IRI *in vivo*. Furthermore, according to another study by Yuan *et al.* (34), acting as a cardiac-protective molecule, miR-145-5p was found to prevent myocardial IRI myocardial by alleviating inflammation and ameliorating apoptosis through negative regulation of the expression of CD40. In addition, Sun *et al.* (35) reported that there was an upregulated expression of miR-145 in H9C2 cells under hypoxic conditions, which was stimulated by HIF-1 α , resulting in a protective effect of miR-145 on cardiomyocytes. The above studies show that miR-145 can provide myocardial protection in reducing cell withering free radical injury and inflammatory response, etc. Moreover, GIGYF1 was predicted to be the target gene of miR-145-5p. Therefore, we speculated that miR-145-5p may be the key miRNA regulating GIGYF1, and regulating the expression level of miR-145-5p may provide protection against IRI through GIGYF1.

Therefore, miR-145-5p may become an endogenous cytoprotective agent to improve IRI through a variety of ways.

In our study, we first verified that intervention on miR-145-5p expression could inhibit excessive apoptosis, promote cell proliferation, and improved H/R injury of cardiomyocytes *in vitro*. Through qRT-PCR detection of a downregulated expression of miR-145-5p in H9C2 cells, our study confirmed the hypothesis that miR-145-5p might play a role in the process of cardiomyocyte H/R and cardiomyocyte proliferation and apoptosis. Besides, based on a successful transfection of miR-145-5p mimic and miR-145-5p inhibitor, CCK8 assay and flow cytometry were performed to detect cell proliferation and apoptosis, SOD test was used to detect the release ability of superoxide dismutase, and ELISA test was used to detect IL-1 β and IL-6 in the supernatant of culture medium, and Western blot was made to detect p-AKT, p53, Bax, p38MAPK and ERK1/2 protein expressions in H9C2 cells. To this end, we elaborated that overexpressing miR-145-5p could enhance H9C2 cell proliferation, improve the release of SOD to accelerate the elimination of oxidative free radicals and improve oxidative stress (36), and upregulate expressions of ERK1/2 and p-AKT, downregulated concentrations of IL-1 β and IL-6 to alleviate inflammation (37), and decreased expressions of P38MAPK, p53 and Bax to prevent cell apoptosis (38). Simultaneously, our experiment further identified the role of intervention on miR-145-5p expression to alleviate myocardial IRI *in vivo*. Since there was IRI based on HE staining and TTC staining in the animal model of IRI, our subsequent experiment had an injection of lentivirus vectors lv-miR-145-5p agomir and negative control lv-agomir-NC into IRI rat model. Consequently and indeed, promoting the expression of miR-145-5p could improve injury degree of heart tissue, increase in the protein expressions of ERK1/2 and p-AKT, downregulate protein expressions of P38MAPK, p53 and Bax. These results suggested that in the IRI rat model, overexpressing miR-145-5p could inhibit excessive apoptosis, promote cell proliferation, and improve myocardial IRI.

Through the miRDB database and TargetScan, our study confirmed that GIGYF1 was the downstream target gene of miR-145-5p. Meanwhile, by referring to the NCBI database, it is found that the protein encoded

by GIGYF1 has a specific GYF domain, which is significantly expressed in myocardial tissue. It can combine with AKT and EGFR to form a macromolecular protein complex, which plays an important role in regulating cell apoptosis (16). Besides, it can bind to Grb10 that can activate tyrosine kinase receptors (such as insulin growth factor receptor and insulin receptor), so as to regulate nutrient metabolism and cell growth and proliferation *in vivo* (17, 18). The latter can also promote the expression of downstream ERK1/2 and promote cell transcription and translation (19). Therefore, GIGYF1 may affect myocardial injury by affecting cell proliferation and apoptosis. In our study, we identified GIGYF1 as the target gene of miR-145-5p. GIGYF1 was a direct binding target of miR-145-5p, and miR-145-5p could inhibit the expression of GIGYF1.

On the basis of the aforementioned findings, in our next experiment, we confirmed that intervention on miR-145-5p expression could inhibit excessive apoptosis, promote cell proliferation, and improve H/R injury of cardiomyocytes *in vitro* via targeting GIGYF1. In order to verify whether miR-145-5p inhibited cardiomyocyte excessive apoptosis, promotes cell proliferation, and improves H/R injury by targeting GIGYF1, H9C2 cells were treated with miR-145-5p mimic alone or miR-145-5p mimic and oe-GIGYF1 together. Western blot detected a downregulated expression of GIGYF1 when overexpressing miR-145-5p, but GIGYF1 expression was increased simultaneous overexpression of miR-145-5p and GIGYF1. Furthermore, with the overexpression of miR-145-5p, there were significantly increased cell proliferation, the improved release of SOD, and upregulated expressions of ERK1/2 and p-AKT; but downregulated concentrations of IL-1 β and IL-6, and decreased expressions of P38MAPK, p53 and Bax; notably, the beneficial roles of overexpressing miR-145-5p were reversed through upregulating GIGYF1 at the same time of overexpressing miR-145-5p. With respect to the above, upregulation of miR-145-5p could downregulate the expression of GIGYF1 targeted; besides, and miR-145-5p overexpression could inhibit excessive apoptosis of cardiomyocytes, promote cell proliferation via silencing GIGYF1 expression targeted, and thus play a protective role in myocardial H/R injury.

In general, through a comprehensive exploration in our study *in vivo* and *in vitro*, our study confirms a decreased expression of miR-145-5p and increased expression of GIGYF1 in the IRI or H/R model. Importantly, overexpression of miR-145-5p can downregulate the expression of GIGYF1, and further promote cell proliferation, inhibit cell apoptosis, alleviate inflammation and oxidative stress, and hence exerts a protective role in myocardial IRI. Findings in our study may contribute to the acceleration of microRNA application clinically and supply a potential reference for the understanding of the pathogenesis mechanism and treatment of myocardial IRI.

Funding

The work was sponsored by the Science Foundation of AMHT (No.: YN202101, Study on the Mechanism of Myocardial Injury under Simulated Microgravity) and the Science Foundation of AMHT (No.: 2020YK01, Physiological Function and Mechanism of Cardiomyocyte-derived Immunoglobulin M in Maintaining Normal Structure and Function of Cardiomyocytes).

References

1. Mlala S, Oyedeji AO, Gondwe M, Oyedeji OO. Ursolic acid and its derivatives as bioactive agents. *Molecules* 2019; 24(15): 2751.
2. Nguyen MT, Kung W-M, Lehman S, Chew DP, Chuang AM-Y, Kung W-M. High-sensitivity troponin in chronic kidney disease: Considerations in myocardial infarction and beyond. *Rev Cardiovasc Med* 2020; 21(2).
3. Cohen MV, Downey JM. What are optimal P2Y12 inhibitor and schedule of administration in patients with acute coronary syndrome? *J Cardiovasc Pharmacol Ther* 2020; 25(2): 121-130.
4. Lee MS, Dahodwala MQ. Percutaneous coronary intervention for acute myocardial infarction due to unprotected left main coronary artery occlusion: status update 2014. *Catheter Cardiovasc Interv* 2015; 85(3): 416-420.
5. Shafiq A, Jang J-S, Kureshi F et al. Predicting likelihood for coronary artery bypass grafting after non-ST-elevation myocardial infarction: finding the best

- prediction model. *Ann Thorac Surg* 2016; 102(4): 1304-1311.
6. Li Y, Chen B, Yang X et al. S100a8/a9 signaling causes mitochondrial dysfunction and cardiomyocyte death in response to ischemic/reperfusion injury. *Circulation* 2019; 140(9): 751-764.
 7. Zhang H, Gong G, Wang P et al. Heart specific knockout of Ndufs4 ameliorates ischemia reperfusion injury. *J Mol Cell Cardiol* 2018; 123: 38-45.
 8. Knight RA, Chen-Scarabelli C, Yuan Z et al. Retracted: Cardiac release of urocortin precedes the occurrence of irreversible myocardial damage in the rat heart exposed to ischemia/reperfusion injury. Elsevier; 2008.
 9. Basso C, Leone O, Rizzo S et al. Pathological features of COVID-19-associated myocardial injury: a multicentre cardiovascular pathology study. *Euro Heart J* 2020; 41(39): 3827-3835.
 10. Tajima T, Yoshifuji A, Matsui A et al. β -hydroxybutyrate attenuates renal ischemia-reperfusion injury through its anti-pyrototic effects. *Kidney Int* 2019; 95(5): 1120-1137.
 11. Guo X, Yin B, Wang C, Huo H, Aziziaram Z. Risk assessment of gastric cancer in the presence of *Helicobacter pylori* cagA and hopQII genes. *Cell Mol Biol* 2021; 67(4): 299-305.
 12. Zhu P, Hu S, Jin Q et al. Ripk3 promotes ER stress-induced necroptosis in cardiac IR injury: a mechanism involving calcium overload/XO/ROS/mPTP pathway. *Redox Biol* 2018; 16: 157-168.
 13. Wu Y, Liu H, Wang X. Cardioprotection of pharmacological postconditioning on myocardial ischemia/reperfusion injury. *Life Sci* 2021; 264: 118628.
 14. Shen Y, Liu X, Shi J, Wu X. Involvement of Nrf2 in myocardial ischemia and reperfusion injury. *Int J Biol Macromol* 2019; 125: 496-502.
 15. Giovannone B, Lee E, Laviola L, Giorgino F, Cleveland KA, Smith RJ. Two novel proteins that are linked to insulin-like growth factor (IGF-I) receptors by the Grb10 adapter and modulate IGF-I signaling. *J Biol Chem* 2003; 278(34): 31564-31573.
 16. Ajiro M, Nishidate T, Katagiri T, Nakamura Y. Critical involvement of RQCD1 in the EGFR-Akt pathway in mammary carcinogenesis. *Int J Oncol* 2010; 37(5): 1085-1093.
 17. Zhou T, Ma Y, Tang J, Guo F, Dong M, Wei Q. Modulation of IGF1R signaling pathway by GIGYF1 in high glucose-induced SHSY-5Y cells. *DNA Cell Biol* 2018; 37(12): 1044-1054.
 18. Zhao Y, Stankovic S, Koprulu M et al. GIGYF1 loss of function is associated with clonal mosaicism and adverse metabolic health. *Nat Commun* 2021; 12(1): 1-6.
 19. Tollenaere MA, Tiedje C, Rasmussen S et al. GIGYF1/2-driven cooperation between ZNF598 and TTP in posttranscriptional regulation of inflammatory signaling. *Cell Rep* 2019; 26(13): 3511-3521. e3514.
 20. Curtis D. Analysis of rare coding variants in 200,000 exome-sequenced subjects reveals novel genetic risk factors for type 2 diabetes. *Diabetes Metab Res Rev* 2022; 38(1): e3482.
 21. Gomes BC, Rueff J, Rodrigues AS. MicroRNAs and cancer drug resistance. *Cancer Drug Resist* 2016: 137-162.
 22. Michlewski G, Cáceres JF. Post-transcriptional control of miRNA biogenesis. *Rna* 2019; 25(1): 1-16.
 23. Kura B, Szeiffova Bacova B, Kalocayova B, Sykora M, Slezak J. Oxidative stress-responsive microRNAs in heart injury. *Int J Mol Sci* 2020; 21(1): 358.
 24. Xing X, Guo S, Zhang G et al. miR-26a-5p protects against myocardial ischemia/reperfusion injury by regulating the PTEN/PI3K/AKT signaling pathway. *Braz J Med Biol Res* 2020; 53.
 25. Wei Z, Qiao S, Zhao J et al. miRNA-181a overexpression in mesenchymal stem cell-derived exosomes influenced inflammatory response after myocardial ischemia-reperfusion injury. *Life Sci* 2019; 232: 116632.
 26. Xiao X, Lu Z, Lin V et al. MicroRNA miR-24-3p reduces apoptosis and regulates Keap1-Nrf2 pathway in mouse cardiomyocytes

- responding to ischemia/reperfusion injury. *Oxid Med Cell Longev* 2018; 2018.
27. Wang H, Zheng X, Jin J et al. LncRNA MALAT1 silencing protects against cerebral ischemia-reperfusion injury through miR-145 to regulate AQP4. *J Biomed Sci* 2020; 27(1): 1-12.
28. Liu W, Miao Y, Zhang L, Xu X, Luan Q. MiR-211 protects cerebral ischemia/reperfusion injury by inhibiting cell apoptosis. *Bioengineered* 2020; 11(1): 189-200.
29. Zhao T, Qiu Z, Gao Y. MiR-137-3p exacerbates the ischemia-reperfusion injured cardiomyocyte apoptosis by targeting KLF15. *Naunyn-Schmiedeberg's Archives of Pharmacology* 2020; 393(6): 1013-1024.
30. Bouquet M, Passmore MR, Hoe LES et al. Development and validation of ELISAs for the quantitation of interleukin (IL)-1 β , IL-6, IL-8 and IL-10 in ovine plasma. *J Immunol Methods* 2020; 486: 112835.
31. Yang J, Liu A, He I, Bai Y. Bioinformatics analysis revealed novel 3' UTR variants associated with intellectual disability. *Genes* 2020; 11(9): 998.
32. Hu S, Cao S, Tong Z, Liu J. FGF21 protects myocardial ischemia-reperfusion injury through reduction of miR-145-mediated autophagy. *Am J Transl Res* 2018; 10(11): 3677.
33. Lin C-M, Fang W-J, Wang B-W et al. (-)-Epigallocatechin Gallate Promotes MicroRNA 145 Expression against Myocardial Hypoxic Injury through Dab2/Wnt3a/ β -catenin. *Am J Chin Med* 2020; 48(02): 341-356.
34. Yuan M, Zhang L, You F et al. MiR-145-5p regulates hypoxia-induced inflammatory response and apoptosis in cardiomyocytes by targeting CD40. *Mol Cell Biochem* 2017; 431(1): 123-131.
35. Sun N, Meng F, Xue N, Pang G, Wang Q, Ma H. Inducible miR-145 expression by HIF-1 α protects cardiomyocytes against apoptosis via regulating SGK1 in simulated myocardial infarction hypoxic microenvironment. *Cardiol J* 2018; 25(2): 268-278.
36. Aruoma OI. Free radicals, oxidative stress, and antioxidants in human health and disease. *J Am Oil Chem Soc* 1998; 75(2): 199-212.
37. Wang X, Guo Z, Ding Z, Mehta JL. Inflammation, autophagy, and apoptosis after myocardial infarction. *J Am Heart Assoc* 2018; 7(9): e008024.
38. Zhao J, Peng W, Ran Y et al. Dysregulated expression of ACTN4 contributes to endothelial cell injury via the activation of the p38-MAPK/p53 apoptosis pathway in preeclampsia. *J Physiol Biochem* 2019; 75(4): 475-487.